Ion Exchange in Ultrathin Films

Timothy W. Graul,† Ming Li, and Joseph B. Schlenoff*

Department of Chemistry and Center for Materials Research and Technology (MARTECH), The Florida State University, Tallahassee, Florida 32306

Received: July 16, 1998; In Final Form: January 19, 1999

Cation exchange in styrene sulfonate gels of thickness less than 100 nm is described. The measurement, involving a radiochemical displacement proximity assay with $^{45}Ca^{2+}$ as a convenient reference ion, permits rapid evaluation of the kinetics and equilibrium distribution of ions. Because the films are so thin, the limiting mechanism for exchange is mass transport through a thin layer of stagnant liquid adjacent to the exchanger, as opposed to mass transport through the exchanger itself, as found with classical resin-based exchanger materials. Thus, equilibrium is quickly established with all cations, including large, hydrophobic ions, which diffuse very slowly through exchanger. Anomalous behavior in this system of well-defined geometry is readily apparent. The technique has sufficient sensitivity such that the thickness of the exchanger can be submonolayer. As an example of the potential for following, in situ, ion exchange at surfaces, a cationic polyelectrolyte is used as solution-phase displacer. The charged segments on the polymer compete with $^{45}Ca^{2+}$ for surface anionic sites. Subtle differences between the adsorption behavior of narrow- and wide-molecular weight distribution polyelectrolyte are revealed.

Introduction

Ion exchange processes are used for purification,[1] decontamination,[2] preconcentration,[3] recovery, metathesis, and separation methods.[4] Ion exchanging membranes have utility as proton conductors in fuel cells.[5] Numerous organic and inorganic[6] materials exhibit ion-exchanging behavior, being composed of a matrix of immobilized charges accessible to solution-phase ions. Organic resinate exchangers are typically based on cross-linked polystyrene derivatives that show selectivity between ions.[7,8] For example, the widely used cation exchanging resins are prepared by sulfonating styrene/divinyl benzene copolymer beads.[9] Studies on the kinetics of sorption and equilibrium distribution of ions are usually performed by flowing a test solution though a column of resin occupied by a reference ion and determining the time-resolved solution concentration of the reference ion.[10−12] For thin film ion exchangers, such as those composed of perfluorinated sulfonated polymers, such measurements can be made on a smaller scale,[13] or electroactive ions can be used as probes when the exchanger coats an electrode.[14,15]

The kinetics of the ion exchange process are generally classified into three rate-limiting mechanisms:[7,16] (1) mass transfer of ions from the external solution phase to the solid exchangers surface though a stagnant film of liquid at the exchanger/fluid interface (film diffusion), (2) diffusion of ions through the solid phase (particle diffusion), and (3) exchange of ions in the vicinity of the exchange groups. Mechanisms 1 or 2 predominate. Previous studies have shown that the pore size of the exchange resin, the size of the ion, and the charge of the ion are all factors in determining the rate of exchange.[10] Most characterization of exchange resins is traditionally done with simple metal ions. Other types of ions are large enough, or have sufficient charge, to severely limit the exchange rate. The diffusion of large, hydrophobic tetraalkylammonium ions, and large dye molecules, though a resin bead is so slow that exchange can take weeks to equilibrate.[10] Specialized techniques have been developed to follow slow exchange. For example, Kim et al.[16] describe confocal fluorescence microspectroscopy on individual laser-trapped exchanger particles to track the movement of Rhodamine dyes through resins.

Other nonclassical exchanging systems, presenting an even greater measurement challenge, include ultrathin layers where the dimension of the exchanger approaches a monolayer. Examples of biological interest include proteins, or synthetic polymers, adsorbing at a charged membrane.[17] In these systems a charged segment displaces a counterion at a charged surface site. Proteins also have strong hydrophilic/hydrophobic interactions but changing even a single charge on a multiply charged macromolecule can have a strong impact on adsorption.[18] While there are various techniques (ellipsometry, surface pressure, neutron reflection, nonlinear optical measurements, surface acoustic wave, and quartz microbalance)[19] available for determining the amount of adsorbed polymer, the small counterions which are exchanged are more difficult to detect. The usual method to enhance signal is to use materials with high specific surface areas such as a powders,[19] but the adsorbate/ion stoichiometry and mechanism are often poorly defined and the surface heterogeneous.

We have recently described a composite material comprised of a block of scintillating plastic coated with a thin cross-linked sulfonated layer.[20] Radiolabeled ions sorbed into the exchanger emit β-particles that traverse the exchanger and impinge the scintillator, which yields a pulse of light. Since the β-particles have limited range, most of the radiolabeled ions in the bulk of solution are unobserved. We demonstrate here that the use of ultrathin films enables rapid equilibration so that even large, hydrophobic ions are quickly transported through the exchanger. Moreover, the sensitivity of the technique is such that ion exchange on a submonolayer scale may be followed with good time resolution.

* Corresponding author.
† Current address: Pfizer Inc., Groton, CT 06340.

10.1021/jp983049o CCC: $18.00
Published on Web 03/24/1999

Experimental Section

The preparation of scintillating polystyrene bearing ultrathin films of polystyrene sulfonate has been described previously.[20] The film thickness, which falls in the range 0.3−10000 nm, is controlled by the concentration of SO_3 in the SO_3/H_2SO_4 mixture used to sulfonate the 2% divinylbenzene crosslinked polystyrene "plastic scintillator."[21,22] Slabs of scintillator (SCSN 81, Kuraray Inc.) of dimensions 1.0 × 1.0 × 0.3 cm^3 were cut from 3 mm sheet. One of the square surfaces was sulfonated by allowing it to come into contact with mixtures of 20% fuming sulfuric acid (Spectrum), and concentrated sulfuric acid (Fisher),[20] followed by rinses in methanol then water. The thickness of styrene sulfonate fell in the range 15−200 dry monolayers (10−150 nm). Polystyrene sulfonated on the surface only was obtained using concentrated H_2SO_4 alone. In this case, the level of sulfonation was approximately 50% of a monolayer.[23]

Metal ion chlorides (LiCl, NaCl, KCl, RbCl, CsCl, and $CaCl_2$, from Fisher, Aldrich or Aesar, all 99% or greater) were dried prior to use. $MgCl_2$, $SrCl_2$, $BaCl_2$, and $CuCl_2$ were obtained from the dried oxides or carbonates by neutralizing with HCl. $CoCl_2$ and $CdCl_2$ were used as received (99.999%, anhydrous, Fisher). YCl_3 (Strem Chemicals) was dissolved in water and assayed gravimetrically as the dried oxide. Tetramethyl-, tetraethyl-, tetrapropyl-, and tetrabutylammonium chloride (Aldrich) were dried under vacuum at 90 °C. Benzyldimethylphenylammonium chloride (Tokyo Kasei) was dried under vacuum at 60 °C. Rhodamine B 610 chloride (Exciton) was used as received. HPLC grade water (Optima, Fisher) was used throughout.

For exchange experiments, ^{45}Ca as $CaCl_2$ (99.90% radiochemical purity, DuPont NEN, ca. 20 Ci g^{-1} specific activity) served as a probe ion. ^{45}Ca is a β-emitter (E_{max} = 0.257 MeV, $t_{1/2}$ = 165 days). The β-particles have an average penetration length though water of about 70 μm (maximum range is 650 μm).[24] Thus, the scintillator detects $^{45}Ca^{2+}$ ions in the thin exchanger layer, and in a thin film of liquid adjacent to the scintillator ("solution background").[25] The solution background is predicted from the geometry of the scintillator, or is experimentally determined at the end of a run by adding a small aliquot of concentrated unlabeled Ca^{2+}, which self-exchanges with any $^{45}Ca^{2+}$ in the sulfonated layer but does not change the solution distribution of $^{45}Ca^{2+}$. Beakers containing 10 mL 10^{-4} M $CaCl_2$ were spiked with 70 μCi $^{45}Ca^{2+}$ to yield a net specific activity of 70 Ci mol^{-1}. The sulfonated cube was added to solution, the beaker was placed above a photomultiplier tube (Hamamatsu R331) in a light-tight box, and the scintillations counted with a Philips PM 6654C Counter interfaced to a computer. The background for this apparatus was 1 or 2 counts per second (cps). A glass stirring rod on the end of a small motor provided constant gentle stirring. For thin films, counts were acquired with 10 or 30 s gate times and were in the range of several thousand per point, reducing counting error to less than 1%.

Exchange of ions at surface-only sulfonated scintillator by solution-phase polyelectrolytes employed 1.2 × 10^{-5} M calcium spiked with 40 μCi $^{45}Ca^{2+}$. The higher specific activity of these systems, about 5 times that of the thin films, ensured a count rate in the range of a few hundred cps, which preserved good counting statistics and time resolution. After the count rate had stabilized, 5 × 10^{-5} M polymer was added. The polymers were either narrow molecular-weight-distribution (MWD) poly(*N*-methyl-2-vinyl pyridinium chloride), PM2VP (M_w = 133,000, M_w/M_n = 1.07), or wide MWD poly(vinyl benzyl trimethylammonium chloride), PVBTA (Scientific Polymer Products, M_w = ca. 10^5, M_w/M_n = 3.1). Both polyelectrolytes carry approximately one strongly dissociated positive charge on each repeat unit.

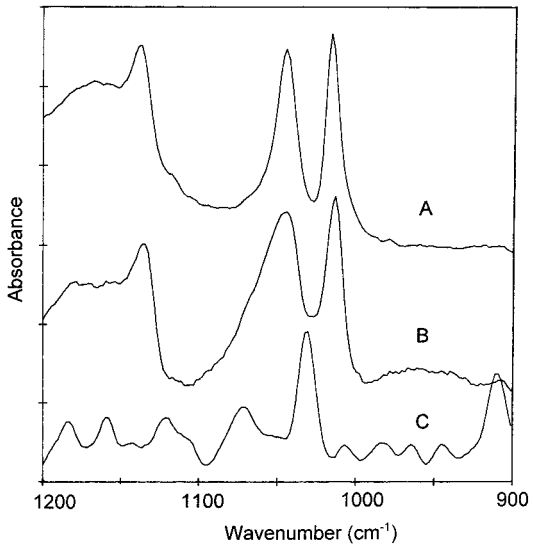

Figure 1. Reflectance FTIR of (A) a drop-cast film of poly(styrenesulfonic acid) on gold foil, (B) a polystyrene scintillator with a 400 nm sulfonated layer, (C) untreated scintillator.

Reflectance−absorption infrared spectra (RAIRS) were acquired with a Nicolet 520 FTIR spectrometer fitted with an Advanced Analytical IR microscope operating in the reflectance mode. The detector was a liquid nitrogen-cooled MCT. For each spectrum, 1000 scans at a resolution of 4 wavenumbers were coadded.

Results and Discussion

Exchange Profiles and Selectivity. The overall ion exchange process can be described by

$$n\mathrm{Ex_2Ca} + 2\mathrm{M}^{n+} \leftrightarrow 2\mathrm{Ex}_n\mathrm{M} + n\mathrm{Ca}^{2+} \qquad (1)$$

The exchanger is a thin layer of sulfonated polystyrene scintillator. Figure 1 depicts the close match between the reflectance FTIR of a piece of scintillator bearing a 400 nm sulfonated film with that of a thin film of polystyrene sulfonic acid drop cast onto gold foil. Our experiments generally involved adding a fixed concentration of $^{45}Ca^{2+}$ as a reference ion, followed by stepwise addition of a competing ion M^{n+}. For example, Figure 2 depicts the count rate vs time of a scintillator with a 150 nm thick sulfonated layer exposed first to unlabeled 10^{-4} M Ca^{2+} (no counts observed) then to a spike (15 μCi) of ^{45}Ca. Following a period of self-exchange (i.e., $M^{n+} = {}^{45}Ca^{2+}$), 1 × 10^{-5} M $BaCl_2$ then 1 × 10^{-4} M $BaCl_2$ were added. After each addition the count rate was allowed to stabilize as equilibrium was reached.

It is possible to screen many ions rapidly using this sensitive technique. The same scintillator could be regenerated by brief exposure to acid (e.g., 1M HCl) or concentrated $CaCl_{2(aq)}$. Exchange using metal ions was generally uncomplicated. For example, the series of alkali metal ions is depicted in Figure 3. The ratio of alkali metal to calcium ion ranged from 10 to 100, since the latter exhibits a much stronger affinity for exchanger. In principle, using this proximity detection scheme, the ion exchange behavior of any material can be measured if it can be deposited on the scintillator as a thin film or layer. The only requirement is that the layer should be thin enough (i.e., less

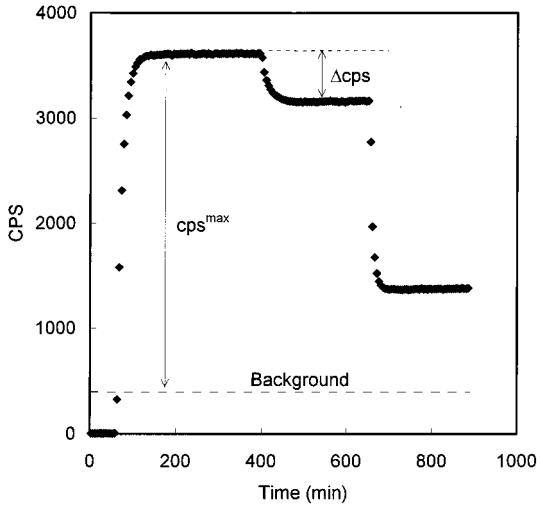

Figure 2. Count rate as a function of time for self-exchange of $^{45}Ca^{2+}$ for Ca^{2+} followed by exchange of $^{45}Ca^{2+}$ with Ba^{2+} using a 150 nm sulfonated layer. At time = 60 min. a spike of $^{45}Ca^{2+}$ was added to 10^{-4} M unlabeled Ca^{2+}. This was followed at $t = 400$ and $t = 650$ min. by the addition of Ba^{2+} bringing the concentration of Ba^{2+} to 1×10^{-5} and 1.1×10^{-4} M, respectively. The solution background contribution was ca. 400 cps.

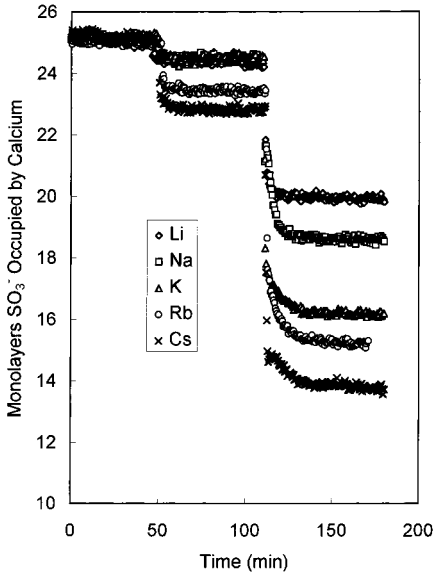

Figure 3. Exchange of Group I ions with 10^{-4} M $^{45}Ca^{2+}$ in a 15 nm thick sulfonated film. The concentration steps correspond to 10 and 100 times the concentration of Ca^{2+}.

than ca. 50 μm for $^{45}Ca^{2+}$) to allow passage of radiation from the radiolabeled probe ion. For example, we have recently monitored ion exchange in polyelectrolyte multilayers.[26−28]

Even very large cations with slow diffusion coefficients, such as rhodamine B, achieved pseudo-steady-state readings within the time (a few hours) of the experiment (see Figure 4), as did large tetraalkylammonium cations (not shown). These ions reach equilibrium rapidly because transport is limited by solution diffusion, rather than particle diffusion, for ultrathin layers, as discussed below. Using our system, anomalous behavior is quickly apparent. For example, after the addition of dye to solution, the count rate for the rhodamine exchange continued to drift slightly, as seen in Figure 4. When the exchanger was soaked in dilute acid to remove the dye, a thin *film* of rhodamine was observed to detach and float away from the surface of the scintillator. The large, planar dye molecule probably associates when concentrated due to stacking-type interactions.

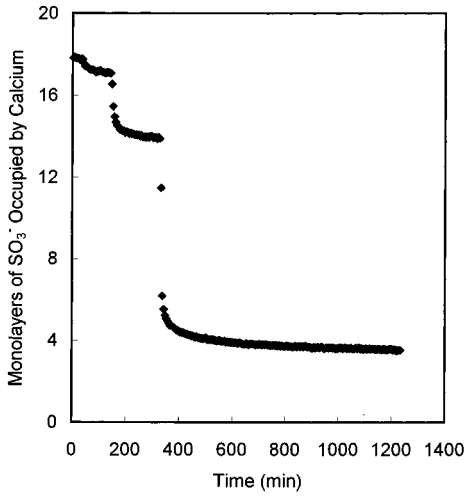

Figure 4. Exchange of $^{45}Ca^{2+}$ with Rhodamine 610. The count rate has been converted to equivalent monolayers of dry SO_3^-. The concentration of $^{45}Ca^{2+}$ is 1.1×10^{-4} M and that for Rhodamine B is 1×10^{-6}, 1.1×10^{-5}, 1.11×10^{-4} M at the various steps.

The selectivity of an exchanger for a particular ion can be defined by several terms. The separation factor α_B^A, useful for demonstrating the preference of one counterion over another, is defined as[7]

$$\alpha_B^A = \frac{\bar{X}_A a_B}{\bar{X}_B a_A} \tag{2}$$

where X_A and X_B are the equivalent ionic fractions of ions A,B in the exchanger, and a_A, a_B are their solution-phase activities. Separation factors for various ions are presented in Table 1.

The selectivity coefficient, K_B^A, for ion A, charge z_A, versus a reference ion B, charge z_B, may also be used to describe ion exchange equilibria:[7,12−14]

$$K_B^A = \frac{\bar{X}_A^{|z_B|} a_B^{|z_A|}}{\bar{X}_B^{|z_A|} a_A^{|z_B|}} \tag{3}$$

As Helfferich points out, K_B^A is not the equilibrium constant for eq 1 as reflected in the concentration dependence of the K_B^As (Table 1).[7] K_B^A merely predicts the constancy of the right-hand term in eq 3 under a given set of conditions. The equilibrium constant[11] includes activity coefficients (unknown) for the exchanger-phase concentration, which would function as concentration-dependent correction factors for eq 3.

The trends in K_B^A are similar to those for classical sulfonated styrene/divinylbenzene systems.[7,11,29−32] The larger ions in a group, those with the smaller solvated equivalent volume, tend to be bound more strongly. A higher charge results in greater affinity for the exchanger due to electrostatic interactions and higher Donnan potentials.[33−35] Within the organic ion series the more hydrophobic the ion the greater its selectivity coefficient. Rhodamine B is particularly effective at displacing calcium.

Polyelectrolyte Adsorption. The lower limit of thickness in the system described herein is a monolayer. When the scintillator was allowed to come into contact with concentrated sulfuric acid containing no SO_3 the surface was sulfonated to the extent of approximately 50% of a monolayer (the precise value varied from 35 to 60% depending on the water content of the concentrated sulfuric acid). This is a charge density of ca. 2×10^{-10} moles charge cm^{-2}. Using ^{45}Ca of high specific activity (in the range of 100−300 Ci mol^{-1}), count rates of about 100

TABLE 1: Selectivities of Ions with Separation Factor and Selectivity Coefficient Using Calcium as the Reference Ion

ion	concentration of Step (M)	$\alpha_B^A(1)$	$\alpha_B^A(2)$	$K_B^A(1)$	$K_B^A(2)$
Li^+	1.1×10^{-3}, 1.11×10^{-2}	1.77×10^{-3}	2.27×10^{-3}	2.64×10^{-2}	3.14×10^{-2}
Na^+	6.0×10^{-4}, 1.06×10^{-2}	2.54×10^{-3}	3.34×10^{-3}	5.50×10^{-2}	6.40×10^{-2}
K^+	6.0×10^{-4}, 1.06×10^{-2}	3.41×10^{-3}	5.08×10^{-3}	9.92×10^{-2}	0.131
Rb^+	1.1×10^{-3}, 1.11×10^{-2}	5.48×10^{-3}	5.76×10^{-3}	0.245	0.161
Cs^+	1.0×10^{-3}, 1.1×10^{-2}	1.04×10^{-2}	7.23×10^{-3}	0.854	0.232
H^+	1.1×10^{-3}, 1.11×10^{-2}	2.80×10^{-3}	2.80×10^{-3}	6.52×10^{-2}	4.51×10^{-2}
Mg^{2+}	1.0×10^{-5}, 1.1×10^{-4}	0.494	0.533	0.243	0.283
Ca^{2+}	1.0×10^{-5}, 1.0×10^{-4}	1.00	1.00	1.00	1.00
Sr^{2+}	1.0×10^{-5}, 1.1×10^{-4}	0.947	1.18	0.899	1.40
Ba^{2+}	1.0×10^{-5}, 1.1×10^{-4}	1.98	1.89	3.93	3.58
Cu^{2+}	1.0×10^{-5}, 1.1×10^{-4}	0.470	0.579	0.221	0.335
Zn^{2+}	1.0×10^{-5}, 1.1×10^{-4}	0.747	0.615	0.559	0.378
Cd^{2+}	1.0×10^{-5}, 1.1×10^{-4}	0.759	0.762	0.577	0.582
Co^{2+}	1.0×10^{-5}, 1.1×10^{-4}	0.582	0.609	0.338	0.371
Y^{3+}	2.0×10^{-7}, 1.2×10^{-6}	15.3	85.8	2.91×10^{-2}	1.75
$(Me)_4N^+$	1.1×10^{-3}, 1.11×10^{-2}	4.97×10^{-3}	5.77×10^{-3}	0.207	0.214
$(Et)_4N^+$	1.1×10^{-3}, 1.11×10^{-2}	8.20×10^{-3}	6.96×10^{-3}	0.546	0.214
$(Pro)_4N^+$	1.1×10^{-3}, 1.11×10^{-2}	9.81×10^{-3}	5.50×10^{-3}	0.768	0.144
$(Bu)_4N^+$	1.1×10^{-3}, 1.11×10^{-2}	1.49×10^{-2}	1.17×10^{-2}	1.79[a]	0.576[a]
$(Be)(Me)_2$ $(Phen)N^+$	1.1×10^{-4}, 1.11×10^{-3}	0.129	0.156	136[a]	87.0[a]
Rhod B	1.1×10^{-5}, 1.11×10^{-4}	2.45	4.07	4.46×10^4 [a]	3.01×10^4 [a]

[a] Activity coefficients not used.

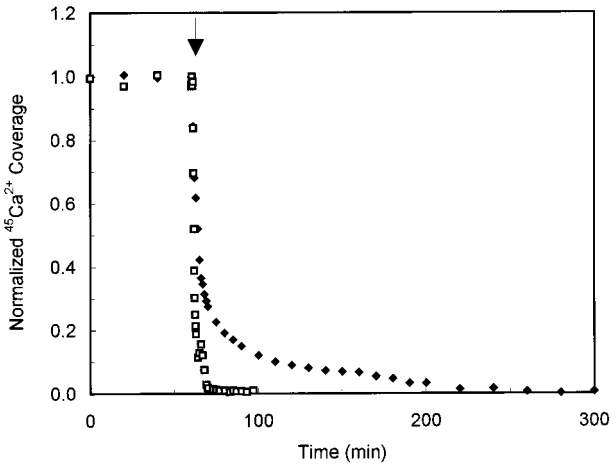

Figure 5. Displacement of $^{45}Ca^{2+}$ from the sulfonated surface of a scintillator by narrow-MWD polyelectrolyte (diamonds) and wide-MWD polyelectrolyte (squares), both 5×10^{-5} M. The concentration of $^{45}Ca^{2+}$ was 1.2×10^{-5} M. Polymer has been added at the point indicated. The coverage of $^{45}Ca^{2+}$ has been normalized, and ranged from 0.35 to 0.55 monolayers (7.2×10^{-11} to 1.1×10^{-10} mol cm^{-2}).

cps could be obtained for surface-bound calcium. Surface exchange with other cations could be easily measured. We were particularly interested in exchange with synthetic polyelectrolytes, where a charged repeat unit on the polymer would compete with $^{45}Ca^{2+}$ for a sulfonate on the surface.[36]

Figure 5 depicts the surface coverage of $^{45}Ca^{2+}$ at surface-sulfonated polystyrene scintillator following the introduction of wide- or narrow-MWD cationic polyelectrolyte. Very efficient displacement of surface $^{45}Ca^{2+}$ is observed. In fact no residual surface concentration of Ca^{2+} was observed (within a detection limit of 2% of a monolayer). This implies efficient surface rearrangement of polyelectrolyte to occupy all sites. In other words, no surface sites sites are "excluded" by irreversible conformation limitations of polymer. There are at least two factors contributing to the high affinity of polymer segments for surface sites. First, the cooperative binding of segments (the polymer can be viewed as a "multidentate" ion with high charge density) leads to strongly favorable adsorption free energy, as is the case with polymer adsorption in general. Second, polymer segments are effectively in high local concentration, as loops dangling off the surface, containing additional positive change, are in close proximity to surface.

There are some interesting differences in behavior between the polymers of different molecular weight distributions (Figure 5). The narrow MWD material exhibits slow displacement of the final 20%, or so, of $^{45}Ca^{2+}$, presumably as segments of the long molecule adjust to occupy all surface sites. In the wide MWD sample, on the other hand, exchange is rapidly complete, probably due to lower molecular weight fractions diffusing in and rearranging faster.

Kinetics. The exchange rate will be limited by diffusion in the exchanger (particle) or by transport though a thin film of stationary liquid next to the solid (film diffusion).[7] A "well stirred" system is commonly achieved for resin beads in the range of 10−1000 μm diameter using flow-through or batch agitation, ensuring particle diffusion is limiting. However, the exchanger employed in the present system is unusually thin. The planar geometry for this system simplifies the treatment of the kinetics of exchange. For particle diffusion control, the fractional attainment of equilibrium f at time t is given by[20,37,38]

$$f = 1 - \frac{16}{\pi^2}\sum_{\nu=0}^{\nu=\infty}\frac{1}{(2\nu+1)^2}\exp\left[-\left(\frac{(2\nu+1)\pi}{h}\right)^2 D_1 t\right] \quad (4)$$

where h is the thickness of the exchanging layer, υ is an integer, and D_1 is the diffusion coefficient in the exchanger. At short time ($f < 0.7$) eq 4 linearizes to

$$f = \frac{2D_1^{1/2}t^{1/2}}{\pi^{1/2}h} \quad (5)$$

The half-time for exchange ($f = 0.5$) $t_{1/2}$ is thus

$$t_{1/2} = \frac{0.196h^2}{D_1} \quad (6)$$

The corresponding expression for the exchange half-time in a

TABLE 2: Theoretical Half-Times of Exchange Assuming Particle Diffusion Comparing a Spherical 100 μm Radius Bead to a Planar 10.7 nm Surface

ion	D_1 ($cm^2\ sec^{-1}$)[37]	$t_{1/2}$ for spherical 100 μm	$t_{1/2}$ for planar 10.7 nm
$(Me)_4N^+$	2.4×10^{-8}	0.52 min	9.35 μs
$(Et)_4N^+$	0.5×10^{-8}	2.5 min	44.9 μs
$(Ben)(Me)_2(Phen)N^+$	6.0×10^{-11}	3.5 h	3.74 ms
Rhod B	3.0×10^{-11}	7.0 h	7.48 ms

spherical bead is

$$t_{1/2} = 0.030\frac{r_0^2}{D_1} \tag{7}$$

Here, r_o is the radius of the exchanger bead. Since a distribution of bead diameters is present in a sample of exchanger resin, an "average" for r_o is commonly employed. For the purposes of comparing classical and ultrathin exchanger morphologies, we estimate the theoretical half-time for various ions in 100 μm spherical and 10 nm planar exchanger in Table 2. It is clear that movement of ions though exchanger in the latter system is rapid and that, since exchange times are many orders of magnitude slower, the limitation here is not particle diffusion.

In the case of film diffusion control the fraction exchanged vs time of ion A in solution with ion B in the exchanger is given by[20]

$$f = 1 - \exp\left(\frac{-D_2C_2t}{h\delta C_1}\right) \tag{8}$$

where D_2 is the solution-phase diffusion, C_2 is the solution concentration of A, δ is the thickness of the stagnant film (on the order of 100 μm), and C_1 is the concentration change in the exchanger. For self-exchange, all available sites are turned over and $C_1 = C^{max}/z_A$, where C^{max} is the total exchanger site concentration. For partial exchange, as in Figures 2−4, $C_1 = yC^{max}/z_A$ where y is the fraction of total sites exchanged during the course of the concentration step. y is obtained from the maximum count rate cps_{max} and the change in count rate during a concentration step Δcps (see Figure 2). With $^{45}Ca^{2+}$ as reference ion, $y = \Delta cps/cps_{max}$, regardless of ion charge. Operationally, f for one of the concentration steps is determined from the count rate at time $= t$, 0, and ∞ as follows:

$$f = 1 - \frac{cps_t - cps_{t=\infty}}{cps_{t=0} - cps_{t=\infty}} \tag{9}$$

The clearest difference between the expressions for particle- and film-diffusion (eqs 5 and 8, respectively) is that the latter depends on solution concentration.

As an example using eq 8 we plotted log(1−f) vs time for self-exchange of Ca^{2+} followed by stepwise addition of 10^{-5} then 10^{-4} M Ba^{2+} in Figure 6. While it appears from eq 8 that the accurate measurement of the parameters δ, h, and C^{max} are required, the quotient $1/h\delta C^{max}$ for a particular sample of exchanger, with reproducible stirring, can be evaluated from the self-exchange data for $^{45}Ca^{2+}$, since the slope of the line is $2D_2C_2/h\delta C^{max}$ and D_2 is known to be 7.9×10^{-6} $cm^2\ s^{-1}$ for Ca^{2+}.[35] Using this quotient and the barium concentrations we determine a diffusion coefficient of 8.7×10^{-6} and 8.0×10^{-6} $cm^2\ s^{-1}$ from the slopes in Figure 6, reasonably close to the literature value of 8.5×10^{-6} $cm^2\ s^{-1}$.[36] An intercept of zero is expected and obtained for the self-exchange. A nonzero intercept

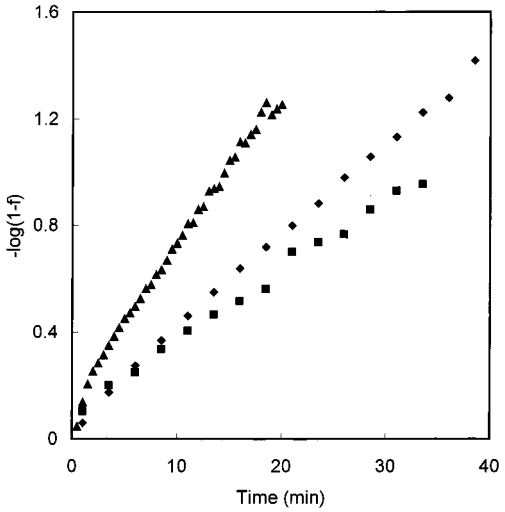

Figure 6. Exchange kinetics from Figure 2 according to eq 8 for self-exchange of $^{45}Ca^{2+}$ (diamonds), followed by stepwise addition of Ba^{2+}, 1×10^{-5} M (squares) and 1.1×10^{-4} M (triangles).

in the case of Ba^{2+} is probably due to the higher density of the spike of $BaCl_2$ added, which fell toward the scintillator before mixing thoroughly.

A detailed kinetic study to yield diffusion coefficients of all ions was not undertaken here, but it should be noted that the time resolution of the technique is expanded for more dilute ions, since exchange is slower and more counts can be acquired per unit time. In conclusion, we have described an ion-exchanging system of well-defined, planar geometry where the exchanging layer is exceptionally thin, enabling rapid equilibration with solution ions. Using this morphology, mass transport is limited by diffusion through a stagnant layer of liquid next to the exchanger. The exceptional sensitivity of the radioanalytical technique employed was demonstrated by following displacement of cations at a surface by an adsorbing polyelectrolyte molecule.

Acknowledgment. This work was supported by Grant DMR 9414289 from the National Science Foundation.

References and Notes

(1) Arden, T. V. *Water Purification by Ion Exchange*; Plenum: New York, 1968.
(2) Bibler, J. P. In *Recent Developments in Ion Exchange*; Williams, P. A., Hudson, M. A., Eds.; Elsevier: London, 1990; pp 121.
(3) Rieman, W.; Walton, H. F. *Ion Exchange in Analytical Chemistry*; Permagon: Oxford, UK, 1970.
(4) Harland, C. E. *Ion Exchange: Theory and Practice*; Royal Society of Chemistry: Cambridge, UK, 1994.
(5) Appleby, A. J.; Foulkes, R. L. *Fuel Cell Handbook*; Van Norstrand, New York, 1989.
(6) Qureshi, M.; Varshney, K. G. *Inorganic Ion Exchangers in Chemical Analysis*; CRC Press: Boca Raton, 1990.
(7) Helfferich, F. *Ion Exchange*; McGraw-Hill: New York, 1962.
(8) Hohenstein, W. P.; Mark, H. *J. Polym. Sci.* **1946**, *1*, 127.
(9) Pepper, K. W. *J. Appl. Chem.* **1951,** *1*, 124.
(10) Kressman, T. R. E. *J. of Phys.Chem.* **1952,** *56*, 118. Kressman, T. R. E.; Kitchener, J. A. *J. Chem. Soc.*, **1949,** 1208.
(11) Bonner, O. D.; Smith, L. L. *J. Phys. Chem.* **1957,** *61*, 326.
(12) Steck, A.; Yeager, H. L. *Anal. Chem.* **1980**, *52*, 1215.
(13) Samec, Z.; Trojanek, A.; Samcova, E. *J. Phys. Chem.*, **1994,** *98*, 6352.
(14) Martin, C. R.; Dollard, K. A. *J. Electroanal. Chem.*, **1983,** *159*, 127.
(15) Szentirmay, M. N.; Martin, C. R. *Anal. Chem.*, **1984,** *56*, 1898.
(16) Kim, H. B.; Hayashi, M.; Nakatani, K.; Kitamura, N.; Sasaki, K.; Hotta, J.; Masuhara, H. *Anal. Chem.* **1996**, *68*, 409.
(17) Sarfert, F. T.; Etzel, M. R. *J. Chromatogr. A* **1997**, *764*, 3.

(18) Ramsden, J. J.; Roush D. J.; Gill, D. S.; Kurrrat R.; Willson, R. C. *J. Am. Chem. Soc*. **1995**, *117*, 8511.
(19) Fleer, G. J.; Cohen Stuart, M. A.; Scheutjens, J. M. H. M.; Cosgrove, T.; Vincent, B. *Polymers at Interfaces*; Chapman and Hall: London, 1993.
(20) Li, M.; Schlenoff, J. B. *Anal. Chem.* **1994,** *66*, 824.
(21) Renschler, C. L.; Harrah, L. A. *Nucl. Instrum. Method.* **1985,** *A235*, 41.
(22) Birks, J. B. *The Theory and Practice of Scintillation Counting*; Permagon: Oxford, UK, 1964.
(23) Schlenoff, J. B.; Ly, H.; Li, M. *J. Am. Chem. Soc.* **1998**, *120*, 7626.
(24) Muramatsu, M. In *Surface and Colloid Science*; Matijevic, E., Ed.; Wiley: New York, 1973.
(25) Wang, R.; Schlenoff, J. B. *Macromolecules* **1998**, *31*, 494.
(26) Schlenoff, J. B.; Li, M. *Ber. Bunsen-Ges. Phys. Chem*. **1996**, *100*, 943.
(27) Schlenoff, J. B.; Wang, R. *PMSE Prepr. ACS Proc.* **1997**, *77*, 654.
(28) Schlenoff, J. B.; Laurent, D.; Ly, H.; Stepp, J. *Adv. Mater.* **1998**, *10*, 347.
(29) Gregor, H. P. J. *Am. Chem. Soc.* **1948,** *70*, 1293.
(30) Gregor, H. P.; Bregman, J. I. *J. Colloid Sci.* **1951,** *6*, 323.
(31) Gregor, H. P.; Frederick, M. *Ann. N.Y. Acad. Sci.*, **1953,** *57*, 87.
(32) Pepper, K. W.; Reichenberg, D. *Z. Elektrochem.* **1953,** *57*, 183
(33) Boyd, G. E.; Schubert, J.; Adamson, A. W. *J. Am. Chem. Soc.* **1947**, *69*, 2818.
(34) Kressman, T. R. E.; Kitchener, J. A. *J. Chem. Soc.* **1949,** 1190.
(35) Pauley, J. L. *J. Am. Chem. Soc.* **1954,** *76*, 1422.
(36) Experiments with thicker sulfonated films showed that polyelectrolytes of molecular weight in the range 10^5 would penetrate no more than about three monolayers of oppositely charged film.
(37) Jost, W. *Diffusion in Solids, Liquids, and Gases*; Academic Press: New York, 1960; pp 37, 45.
(38) Schlenoff, J. B., Chien, J. C. W. *J. Am. Chem. Soc.* **1987,** *109*, 6269.
(39) Mills, R.; Lobo, V. M. M. *Self-Diffusion in Electrolyte Solutions*; Elsevier: Amsterdam, 1989; p 50.
(40) Kressman, T. R. E.; Kitchner, J. A. *Disk. Farad. Soc.* **1949**, *7*, 95.